Journal of Physics: Conference Series **548** (2014) 012016 doi:10.1088/1742-6596/548/1/012016

Resonant four-wave mixing spectra: A fresh look at photodissociation dynamics

A Kouzov[1], P Radi[2], P Maksyutenko[2], and D Kozlov[3]

[1]Saint-Petersburg State University, 198504 Saint-Petersburg, Russia
[2]Paul Scherrer Insitute, 5232 Villigen, Switzerland
[3]A.M. Prokhorov General Physics Institute, 119991 Moscow, Russia

E-mail: alex@ak1197.spb.edu, peter.radi@psi.ch, pavlo.maksyutenko@gmail.com, dnk@kapella.gpi.ru

Abstract. Frequency- and polarization-resolved degenerate resonant four-wave mixing is used for the first time to study the rotational anisotropy of the OH radicals produced by photolysis of H_2O_2 by a plane-polarized laser radiation at 266 nm. For that, a flexible polarization setup is designed to directly isolate the rotationally anisotropic signals in the $A^2\Sigma^+ - X^2\Pi(0,0)$ OH vibronic band. The results are quantitatively interpreted by using the line-space approach and accounting for all possible correlations between the electric field $\mathbf{E}_D$ of the photolysis laser, the recoil velocity $\mathbf{v}$ and the angular momentum $\mathbf{J}$ of nascent particles. In so doing, the resonance amplitudes are decoupled into products of the polarization factors, the Doppler-broadened profiles and the Einstein B-coefficients. The anisotropic signals have characteristic shapes of well resolved Doppler doublets providing a direct evidence of translational helicity of the nascent OH radicals, a hitherto expremental inaccessible key characteristic of the photodissociation path.

1. Introduction

The photodissociation reaction $AB \xrightarrow{\hbar\omega_D} A + B$ has a paramount importance for theoretical chemistry, for its understanding can shed light on the final stage of reactive collisions [1]. Advantageously, the reaction is naturally controlled by the photolysis laser intensity I_D and, what is by far more important, by the frequency ω_D and polarization $\mathbf{e}_D$. Here, we shall consider only moderate intensities whose variation has a minute effect on the reaction dynamics and results only in a linear scale of the production rate. Conversely, the energy ($\hbar\omega_D$) and the polarization of an absorbed photon affect the reaction path and, therefore, are strongly imprinted on the properties of the nascent particles A and B. Due to the basic inseparability principle [2], the wave functions of A and B are always unknown linear combinations of eigenvectors of the free species. In other words, the quantum states of products are correlated and this correlation is given in terms of their density matrices ρ^A and ρ^B, the most detailed observable characteristics of the photolytic reaction which can be obtained by studying the nascent particles. The strongest correlations arise between the $(2J+1)$-degenerate substates of products corresponding to different space orientations of their total angular momenta $\mathbf{J}_n$ $(n = A, B)$. To describe the effect, the so-called state multipoles ρ^n_K $(K = 0, 1, 2...)$ are introduced [2], with the monopole term $(K = 0)$ corresponding to the completely chaotic (isotropic) $\mathbf{J}_n-$orientation and the others characterizing the reaction-induced rotational anisotropy.

An impressive progress achieved so far in purely optical studies of photofragments almost entirely owes to the use of laser-induced fluoresence (LIF) [1]. However, a LIF setup operates with two polarizations and, because of this, the detected signal is informative only on the K =0,2,4 state multipoles [3]. Advantageously, four polarizations are controllable if one uses the Resonant Four-Wave Mixing (RFWM) techniques. Due to this sophistication, all state multipoles with $K \leq 4$ contribute to the (coherent) response thus allowing a deeper insight into the reaction path.

Here, we provide the reader with further details omitted in our previous paper [4] on degenerate RFWM (i.e. one-color or DFWM) spectra of the OH radicals produced by laser photolysis of H_2O_2 molecules at 266 nm.

2. Outline of theory

The symbol m denotes a collection of the principle quantum numbers (including also the total angular momentum J_m) which defines the photofragment eigenstate. Omitting for brevity the photofragment label, the rotational anisotropy of the state m can be generally introduced with the help of the irreducible tensor operators

$$N_Q^{(K)}(m) = \rho_{mm}^{-1/2} \sum_{M_m M'_m} (-1)^{J_m - M_m} C^{KQ}_{J_m M_m J_m - M'_m} \mid mM_m\rangle\langle mM'_m \mid \tag{1}$$

where $C^{KQ}_{J_m M_m J_m M'_m}$ are the Clebsch-Gordan coefficients and ρ_{mm} is the total Boltzmann factor of the state m, i.e. its total population divided by $2J_m + 1$. Using Dixon's approach [5] to account for the anisotropic distribution of the translational velocity $\mathbf{v} =(v, \Omega_v)$, we obtain

$$\rho = \sum_{mKL\lambda} t^{(m)}_{KL\lambda}(\{C^{(\lambda)}(\Omega_D) \otimes C^{(L)}(\Omega_v)\}^{(K)}, N^{(K)}(m)) \tag{2}$$

where $C^{(l)}_\sigma$ ($\sigma = -l, -l+1, ..l$) are the Racah spherical harmonics; the outer parentheses and the braces respectively denote the scalar and tensor contraction operations [6]; Ω_D is the orientation of the polarization plane $\mathbf{e}_D$ of the photolysis laser beam in the laboratory frame (X, Y, Z), with OZ assumedly coinciding with the beam wave vector. Besides, only the ranks $\lambda = 0, 2$ are allowed in (2). The coefficients $t^{(m)}_{KL\lambda}$ are proportional to the statistical weights of the velocity- and state-dependent correlations imposed on the nascent molecules by the electric field $\mathbf{E}_D(= E_D\mathbf{e}_D)$. The $\lambda = K = L = 0$ term refers to the isotropic case for which the $\mathbf{v}$- and $\mathbf{J}-$orientations are completely chaotic. The remaining terms with $\lambda = 0$ describe the mutual $\mathbf{v} - \mathbf{J}$ correlations of order one, the helicity effect for which $K = L = 1$ and $\mathbf{v}$ and $\mathbf{J}$ can be either parallel or antiparallel. At $\lambda = 0$, the alignment $K = L = 2$ terms may also contribute as well as the higher-order ones ($K = L = 3, 4, ..$), all independent on the photolysis laser polarization. In the $\lambda = 2$ case, the effects relate to the field direction and include the double $\mathbf{E}_D - \mathbf{v}$ (for which $K = 0$ and $L = 2$) and $\mathbf{E}_D - \mathbf{J}$ ($L = 0, K = 2$) alignment terms as well as the triple ($\mathbf{E}_D - \mathbf{v} - \mathbf{J}$) ones when both K and L are distinct from zero. Of particular importance is the field-induced helicity contribution, i.e. the term with $\lambda = 2, K = L = 1$.

The key quantity targeted by the RFWM theory is the resonance part of the third-order susceptibility, $\chi^{(res)}$. As in the isotropic case [7], the line-space formalism appears to be an efficient tool to study this quantity. Another salient feature of our approach is the velocity averaging which was analytically performed in the limit when the photon energy $\hbar\omega_D$ much exceeds the dissociation threshold ε_D. In this limit, the kinetic energy T of a nascent OH radical is almost fixed, $T = (\hbar\omega_D - \varepsilon_D)/2 = m_{OH}v^2/2$, and the role of the Doppler effect on the RFWM shapes is paramount. After tedious tensor recouplings, the final result reads

$$\chi^{(res)} = \rho_{ii} \sum_{\lambda KL} t^{(i)}_{KL\lambda} \sum_{r_1 r_2} B^2_{if} F(J_i, J_f; r_1, r_2, K)\{C^{(\lambda)}(\Omega_D) \otimes G^{(K)}(r_1, r_2)\}^{(L)}_0 \Phi_L(\Delta\Omega/kv) \tag{3}$$

where B_{if} is the Einstein B-coefficient for the pumped transition. Here, $G^{(K)}_{\sigma} = \{\{e^{(1)}_1 \otimes e^{(1)*}_2\}^{(r_1)} \otimes \{e^{(1)}_3 \otimes e^{(1)*}_4\}^{(r_2)}\}^{(K)}_{\sigma}$ $(\sigma = -K, -K+1, ...K)$ is the spherical tensor built on the polarization unit vectors $\mathbf{e_n} \equiv e^{(1)}_n$ $(n = 1, 2, 3, 4)$ of the DFWM beams. At detunings $|\Delta\Omega|$ from the resonance frequency ω_{fi} which do not exceed $kv = \omega_{fi}v/c$, the shape function $\Phi_L(\Delta\Omega/kv)$ coincides with the Legendre polynomial P_L of the same argument; otherwise, $\Phi_L = 0$. Structurally, Eq. (3) reproduces the result of Wasserman et al [8, 9] who treated the anisotropy induced by optical pumping; however, the $F-$coefficients derived by us contain also $9j$-symbols missing in the previously derived formuli [9].

The DFWM technique allows a handy way to separate the signal entirely induced by anisotropy from the by far dominating "isotropic" background term proportional to the state monopole $t^{(i)}_{000}$. For that, the input beams 1,2,3 are to be polarized along OY and the signal channel polarizer should be aligned with OX, that is shortly denoted as $(\mathbf{e}_1, \mathbf{e}_2, \mathbf{e}_3, \mathbf{e}_4) = YYYX$. Equation (3) can be used to analyze $\chi^{(res)}$ as a function of the angle φ between $\mathbf{e}_D$ and OX. In so doing, we obtain

$$\begin{aligned}\chi^{(res)} &= i[a_1\Phi_1(\Delta\Omega/kv) + a_3\Phi_3(\Delta\Omega/kv)] + i[b_1\Phi_1(\Delta\Omega/kv) + b_3\Phi_3(\Delta\Omega/kv)]\sin 2\varphi \\ &+ [c_0\Phi_0(\Delta\Omega/kv) + c_2\Phi_2(\Delta\Omega/kv) + c_4\Phi_4(\Delta\Omega/kv)]\cos 2\varphi \end{aligned} \quad (4)$$

where the φ-independent terms are proportional to $t^{(i)}_{110}$ and $t^{(i)}_{330}$, correspondingly. Similarly, b_1 and b_3 correspond to the field-induced odd-rank anisotropies characterized by $t^{(i)}_{112}$ and $t^{(i)}_{332}$. Finally, the terms varying as $\cos 2\varphi$ are, respectively, proportional to $t^{(i)}_{202}, t^{(i)}_{222}$ and $t^{(i)}_{242}$ and thus refer to the binary $\mathbf{E}-\mathbf{J}$ and triple $\mathbf{E}-\mathbf{J}-\mathbf{v}$ correlations. Since all coefficients a, b and c are real quantities and the intensity I is proportional to $|\chi^{(res)}|^2$, the interference between the terms proportional to the odd- and even-order Legendre polynomials is forbidden and, therefore, the observable shapes appear to be even functions of $\Delta\Omega$. Since for odd orders $P_L(0) = 0$, the $YYYX$ profiles measured at $\varphi = \pi/4$ in a collisionless medium should have a vanishing intensity at $\Delta\Omega = 0$ provided that all nascent particles have the same recoil velocity v. In the simplest case when only the a_1- and b_1-terms are of importance, all anisotropic profiles should behave as $\Delta\Omega^2$ at $|\Delta\Omega| \leq kv$ and disappear at higher detunings.

3. Experimental detalis

The forward-box geometry of DFWM was used, for which all the laser beams, including that of the photolysis laser, were almost co-propagating along OZ. While the photolysis laser wavelength was fixed at 266 nm, the (common) frequency of the input and output beams was scanned that allowed to study the DFWM resonances in the $A^2\Sigma^+ - X^2\Pi(0,0)$ OH vibronic band with resolution of about 0.1 cm^{-1}. All spectra were recorded by applying laser pulses with durations of 6 ns. The reader is referred to our previous publication [4] where the DFWM setup is explicitly described.

Results of two series of low-pressure experiments ($p \leq 1$ mbar) are presently reported. In the first series, no delay was introduced between the dissociation and pump/probe pulses and the $YYYX$ responses were measured for different angles φ. Second, the DFWM pulses were delayed by time t_d and the anisotropic signals were studied as function of $t_d \leq 100$ ns at $\varphi = \pi/4$. Estimations show that the results obtained in the first series of experiments can be interpreted assuming the absence of collisions at times not longer than the pulse durations. However, at delays longer than few tens of ns the signals appear to dramatically change with t_d demonstrating the increasing role of collisions in this time scale.

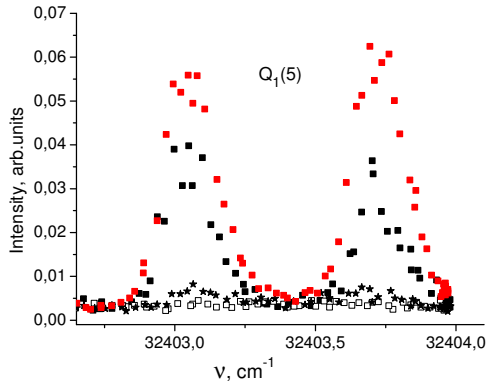

Figure 1. $Q_1(5)(0-0)$ profiles at YYYX geometry for different angles φ between dissociation laser polarization and OX: (black squares) $\varphi = -\pi/4$; (red squares) $\varphi = \pi/4$; (empty squares) $\varphi = 0$; (stars) $\varphi = \pi/2$

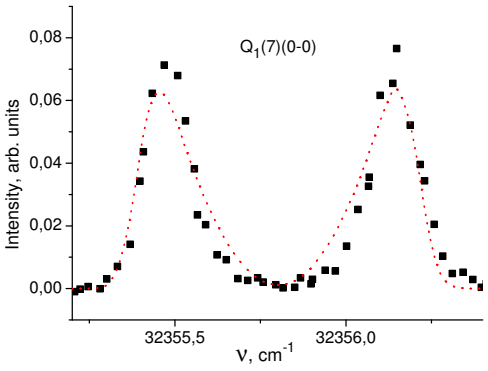

Figure 2. Experimental anisotropic YYYX shape of $Q_1(7)(0-0)$ line at $\varphi = -\pi/4$ (squares) and its theoretical fit (dashed line).

4. Discussion

Four plots in Fig. 1 show how the $Q_1(5)$ shape is altered by variations of φ. Equation (4) shows that the even-order polynomials do not contribute to I at $\varphi = \pm\pi/4$. Since the intensity is tangibly changed when φ is switched between these angles, we conclude that this variation should be assigned to interference between the terms of $\chi^{(res)}$ proportional to the $a-$ and $b-$ coefficients. Besides, the intensity almost vanishes at $\varphi = 0$ showing that the squares of the $a-$ and $c-$terms do not practically contribute to I. However, I is strongly enhanced when φ is set equal to $\pm\pi/4$ which implies the predominance of the b-terms while the $a-$ ones play a minor role. Furthermore, based on the fact that $I(\pi/4) > I(-\pi/4)$, we conclude the a and b coefficients to be of the same sign. Since the correlations are known to rapidly decrease with their orders, the a_1 and b_1 terms are the most important ones. Recall that the smaller a_1-term refers to the $\mathbf{v} - \mathbf{J}$ correlation not subjected to the orientation of $\mathbf{e}_D$, while the b_1-term originates because of the triple $(\mathbf{E}_D - \mathbf{v} - \mathbf{J})$ correlations. Both terms are caused by the helicity effect for which the mean value of $\cos(\mathbf{v}, \mathbf{J})$ is distinct from zero. In other words, some of the OH radicals move like bullets rotating either clockwise or counterclockwise along the trajectory direction.

The existence of helicity finds further support from the analysis of the anisotropic signal shapes. The theory based on Eq. (4) predicts the measured profiles to be well-resolved doublets with an almost zero intensity in the center. A good agreement between theory and experiment is demonstrated by Figure 2 where the simulated and experimental profiles of the $Q_1(7)$ line are depicted. The parabolic theoretical shape $\Delta\Omega^2$ was cut off at $|\Delta\Omega| = kv$ and then convolved with the Gaussian line to account for the finite laser line width and for the recoil velocity dispersion. Fittings resulted in the Gaussian FWHH=0.12 cm^{-1} and kv =0.42 cm^{-1}, in a reasonable accord with estimations of these parameters.

To the best of our knowledge, the rotation-translation helicity of the photolysis products is a new effect which has not been detected so far by using purely optical means. The proof of helicity is a new step in the investigation of photolytic decomposition of H_2O_2 for which a pronounced rotation-translation alignment has been already established. However, the knowledge of alignment can not help us to distinguish between the clockwise and

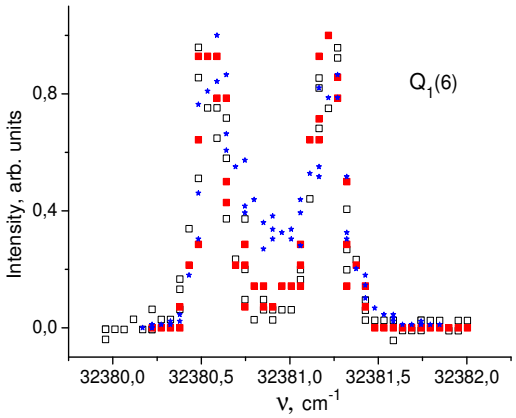

Figure 3. Transformation of the normalized YYYX $Q_1(6)(0-0)$ profiles (p=0.5 mbar) with dissociation-probe delay time t: (empty squares) $t = 0$ ns; (red squares) $t = 20$ ns; (blue stars) $t = 50$ ns. Intensities at t=20 ns and t=50 ns were magnified by factors 2 and 8, correspondingly

counterclockwise rotations whereas a nonzero helicity proves that the OH radicals are rotating only in one direction. Unfortunately, we are yet unable to find out which direction is realized since upon squaring of $\chi^{(res)}$ the information on the helicity sign is lost. To resolve the issue, an implementation of other RFWM techniques for which a useful signal scales linearly with $\chi^{(res)}$ is required.

Another series of experiments was performed with a varied delay time t_d between the pulses of the dissociation and DFWM lasers. Due to the delay, the rotational anisotropy is increasingly lost with t_d. Indeed, as seen from Fig. 3, the $Q_1(6)$ anisotropic signal becomes eight times weaker upon the 50 ns delay showing considerable randomization of the rotational momentum orientation. Also, smoothing of the signal shape with increasing t_d is evident from Fig. 3 that gradually fills the gap between the doublet components. This effect can be explained by velocity changing collisions which cause the spectral exchange and the intensity transfer to the doublet center. However, the overall Doppler width which correlates with v is not visibly affected. Therefore, we may conclude that the absolute value of the recoil velocity does not considerably vary at the time scale of 50 ns whereas the orientation of $\mathbf{v}$ becomes tangibly randomized by elastic collisions.

Acknowledgements

Support from the Science and Technology Cooperation Program Switzerland-Russia (GA 128546), the Swiss Federal Office of Energy, the Swiss National Science Foundation (# 200020_146387) and from the Russian Foundation for Basic Research, grants #15-02-05290 and # 15-03-04997, is gratefully acknowledged.

References

[1] Sato H 2001 *Chem. Rev.* **101** 2687
[2] Blum K 2012 *Density Matrix. Theory and Applications* (Berlin: Springer)
[3] Greene C H and Zare R N 1983 *J. Chem. Phys.* **78** 6741
[4] Maksyutenko P, Radi P P, Kozlov D N, and Kouzov A P 2013 *J. Raman Spectrosc.* **44** 1349
[5] Dixon R N 1986 *J. Chem. Phys.* **85** 1866
[6] Varshalovich D A, Moskalev A N, and Khersonskii V K 1988 *Quantum Theory of Angular Momentum* (Singapore: World Scientific)
[7] Kouzov A and Radi P 2014 *J. Chem. Phys.* **140** 194302
[8] Wasserman T A W, Vaccaro P H, and Johnson B R 1997 *J. Chem. Phys.* **106** 6314
[9] Wasserman T A W, Vaccaro P H, and Johnson B R 1997 *J. Chem. Phys.* **108** 7713